

Electronic Supplementary Information

Chromium nitride as stable cathode current collector for thin film all-solid-state Li-ion batteries

Alejandro N. Filippin,^{†*1} Michael Rawlence,^{†1} Aneliia Wäckerlin,¹ Thomas Feurer,¹ Tanja Zünd,^{1,2} Kostiantyn Kravchyk,^{1,2} Maksym V. Kovalenko,^{1,2} Yaroslav E. Romanyuk,¹ Ayodhya N. Tiwari,¹ Stephan Buecheler^{*1}

¹ Laboratory for Thin Films and Photovoltaics, Empa - Swiss Federal Laboratories for Materials Science and Technology, Überlandstrasse 129, CH-8600 Dübendorf, Switzerland.

² Laboratory of Inorganic Chemistry, ETH Zürich, Vladimir Prelog Weg 1, CH-8093 Zürich, Switzerland

*contact e-mail: alejandro.filippin@empa.ch, Stephan.Buecheler@empa.ch

† Indicates co-first author

Experimental

The coin cells used in this work were assembled according to the scheme presented in Fig. S1.

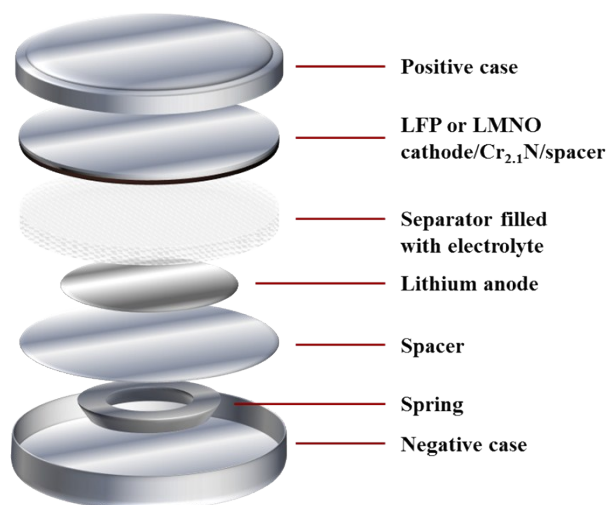


Figure S1. Scheme of the coin cells assembly.

Results and discussion

The thickness of the Cr_xN films with varying N₂/Ar content is presented in Fig. S2. The thickness was calculated from SEM cross sections (Fig. S4).

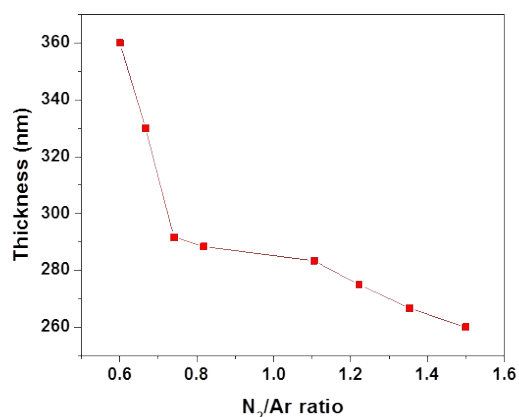


Figure S2. Cr_xN thin film thickness determined by SEM as a function of the N₂/Ar ratio.

Table ST1. Quantification values of the different Cr_xN samples from the EDX spectra. The penetration depth of the electrons is larger than the Cr_xN films, therefore we observe aluminum, sodium, magnesium and silicon signals which originate from the soda lime glass used as substrate.

N ₂ /Ar ratio	Element	Atomic Number	Netto	Mass (%)	Mass Norm. (%)	Atomic (%)	Abs. error (%)	Rel. error (%)
1.50	Nitrogen	7	42815	19.24	18.28	40.01	2.32	12.06
	Oxygen	8	15432	5.48	5.20	9.97	0.75	13.68
	Sodium	11	2789	0.61	0.57	0.77	0.07	10.75
	Silicon	14	26892	5.18	4.92	5.38	0.24	4.63
	Chromium	24	64405	73.51	69.84	41.17	2.78	3.78
	Carbon	6	2014	1.00	0.95	2.42	0.21	21.42
	Magnesium	12	1281	0.22	0.21	0.27	0.04	17.77
	Aluminium	13	138	0.02	0.02	0.02	0.00	11.21
			Sum	105.26	100.00	100.00		
1.35	Nitrogen	7	33793	18.34	17.79	39.65	2.26	12.31
	Oxygen	8	11318	4.84	4.69	9.16	0.69	14.28
	Sodium	11	1648	0.47	0.45	0.61	0.06	12.41
	Silicon	14	17464	4.60	4.46	4.96	0.22	4.74
	Chromium	24	53197	73.58	71.38	42.85	2.79	3.79
	Carbon	6	1605	0.95	0.92	2.40	0.22	22.61
	Magnesium	12	895	0.20	0.20	0.26	0.04	19.16
	Aluminium	13	460	0.10	0.09	0.11	0.03	33.38
			Sum	103.08	100.00	100.00		
1.22	Nitrogen	7	33415	16.88	16.44	37.82	2.08	12.34
	Oxygen	8	11383	4.41	4.30	8.65	0.63	14.32
	Sodium	11	1674	0.46	0.45	0.63	0.06	12.43
	Silicon	14	16509	4.12	4.02	4.61	0.20	4.81
	Chromium	24	58872	75.74	73.74	45.71	2.87	3.79
	Magnesium	12	748	0.16	0.16	0.21	0.04	22.79
	Carbon	6	1620	0.89	0.87	2.34	0.20	22.73

	Aluminium	13	156	0.03	0.03	0.04	0.00	10.72
			Sum	102.71	100.00	100.00		
1.11	Nitrogen	7	39105	16.20	15.61	36.60	1.97	12.18
	Oxygen	8	16235	5.12	4.93	10.12	0.70	13.63
	Sodium	11	2534	0.56	0.54	0.77	0.06	11.13
	Silicon	14	24053	4.87	4.69	5.48	0.23	4.68
	Chromium	24	71261	76.37	73.59	46.47	2.89	3.78
	Magnesium	12	1273	0.22	0.21	0.29	0.04	17.87
	Aluminium	13	510	0.08	0.08	0.10	0.03	38.01
	Copper	29	637	0.36	0.35	0.18	0.12	32.82
				Sum	103.78	100.00	100.00	
0.82	Nitrogen	7	36722	13.93	13.51	33.46	1.71	12.27
	Oxygen	8	14033	3.85	3.73	8.10	0.54	14.03
	Sodium	11	857	0.17	0.16	0.25	0.04	22.54
	Silicon	14	16707	3.19	3.09	3.82	0.16	4.99
	Chromium	24	83468	80.59	78.18	52.15	3.04	3.77
	Copper	29	975	0.51	0.49	0.27	0.14	27.75
	Magnesium	12	931	0.15	0.14	0.21	0.04	23.64
	Aluminium	13	903	0.14	0.14	0.17	0.03	24.23
	Carbon	6	1350	0.56	0.55	1.58	0.14	25.32
			Sum	103.09	100.00	100.00		
0.74	Nitrogen	7	28915	12.61	12.63	31.96	1.58	12.55
	Silicon	14	12844	2.55	2.55	3.22	0.13	5.23
	Chromium	24	69667	80.42	80.49	54.88	3.04	3.78
	Oxygen	8	10175	3.21	3.22	7.13	0.47	14.74
	Sodium	11	1065	0.23	0.23	0.35	0.04	18.60
	Magnesium	12	619	0.10	0.10	0.15	0.03	31.87
	Carbon	6	1533	0.78	0.78	2.31	0.18	23.42
				Sum	99.90	100.00	100.00	
0.66	Nitrogen	7	29381	12.19	11.74	30.76	1.53	12.54
	Silicon	14	8880	1.64	1.58	2.06	0.10	5.85
	Chromium	24	80302	86.18	83.01	58.57	3.25	3.77
	Oxygen	8	11414	3.32	3.20	7.33	0.48	14.50
	Carbon	6	816	0.37	0.36	1.09	0.11	30.73
	Sodium	11	554	0.11	0.11	0.18	0.03	30.44
				Sum	103.82	100.00	100.00	
0.60	Nitrogen	7	30319	10.95	10.75	28.70	1.37	12.53
	Silicon	14	10259	1.73	1.70	2.26	0.10	5.74
	Chromium	24	92638	85.00	83.40	60.01	3.20	3.77
	Oxygen	8	13007	3.09	3.04	7.10	0.44	14.32
	Copper	29	1189	0.60	0.59	0.35	0.15	25.76
	Carbon	6	1253	0.50	0.49	1.52	0.13	26.34
	Aluminium	13	388	0.05	0.05	0.07	0.03	56.56
	Magnesium	12	0	0.00	0.00	0.00	0.00	3.05
				Sum	101.92	100.00	100.00	

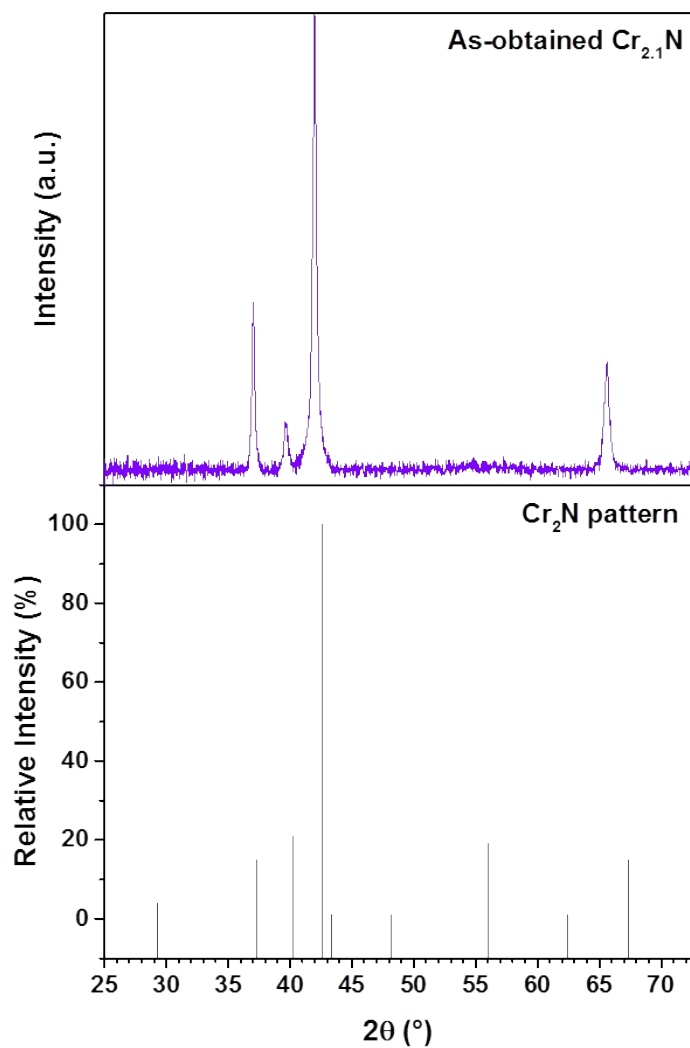


Figure S3. Relative peaks intensities of as-prepared Cr_{2.1}N (top) and the Cr₂N pattern.

The SEM cross sections in Fig. S4 were obtained by mechanical cleaving of the silicon substrate.

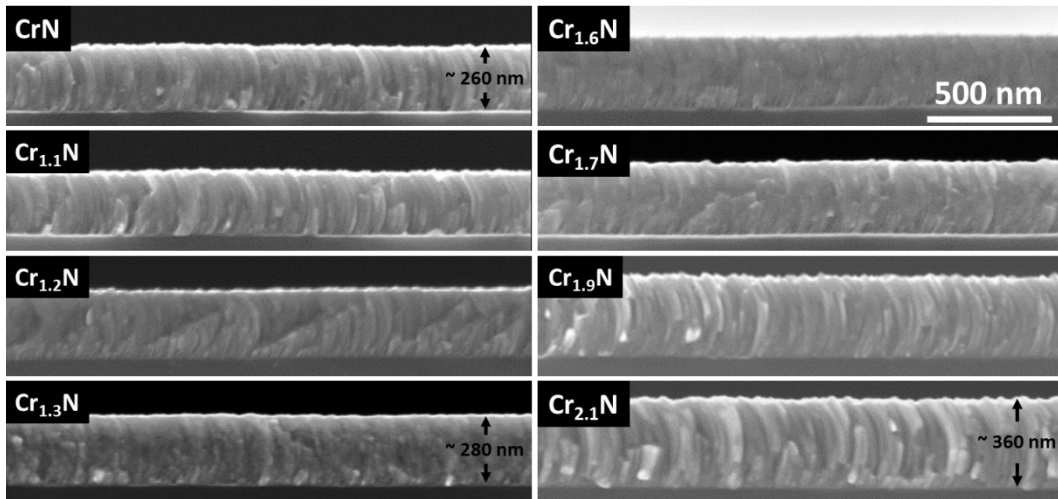


Figure S4. SEM cross sections of Cr_xN thin films on Si(100).

The change in surface microstructure for CrN-Cr_{2.1}N is presented in Figure S5.

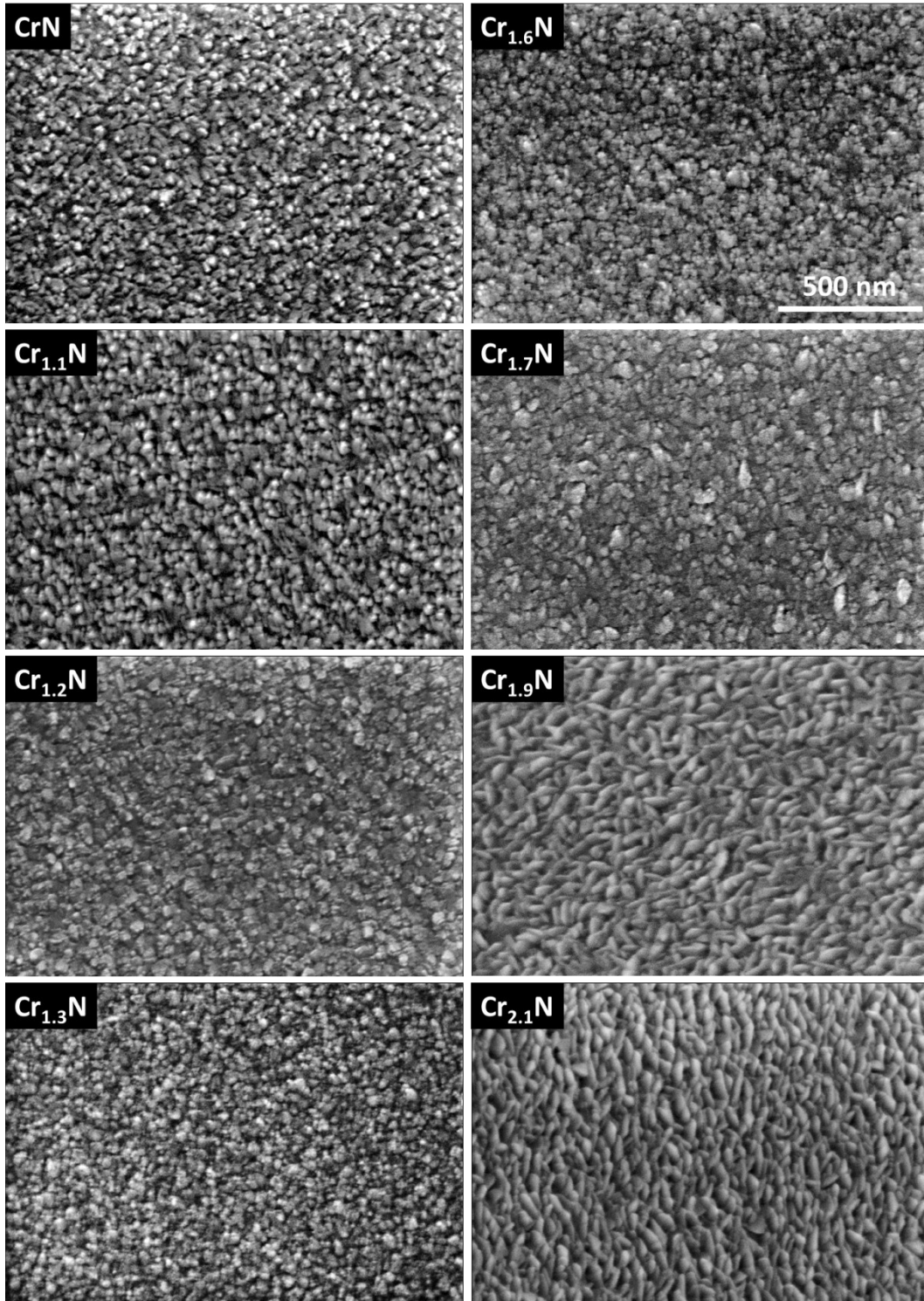


Figure S5. SEM normal views of Cr_xN thin films (the scale is the same for all images).

For the $\text{Cr}_{2.1}\text{N}$ composition, the thickness of the film was swept between 45 nm and 489 nm, Fig. S6, and the sheet resistance measured as shown in Fig. S6a), obtaining an exponential trend for the sheet resistance that approximately obeys the equation $sh = 2.79 + 39.56 \times e^{-0.01 \times th}$ [$R^2 = 0.992$], where sh is the sheet resistance and th the thickness. Even for the thinnest film prepared of 45 nm the sheet

resistance remains relatively low and from the SEM micrographs of Fig. S7(b-d) no macroscopic voids are observed, although this low thickness region is characterized by the presence of discontinuities or islands in the film.

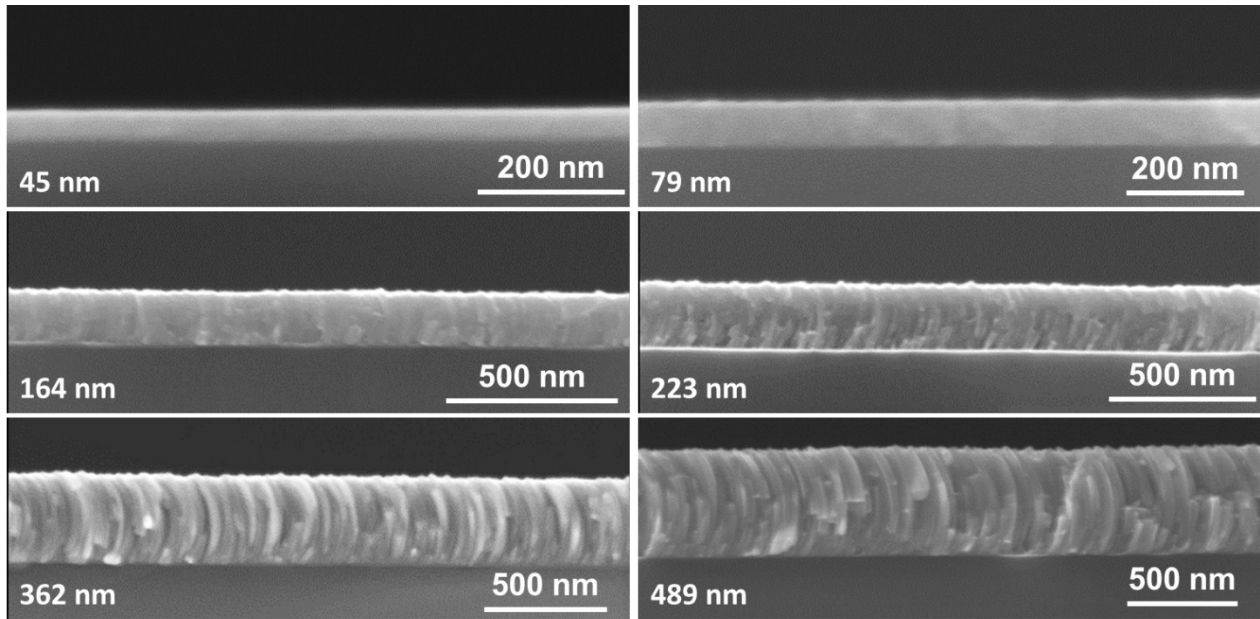


Figure S6. SEM cross sections of $\text{Cr}_{2.1}\text{N}$ with different thicknesses.

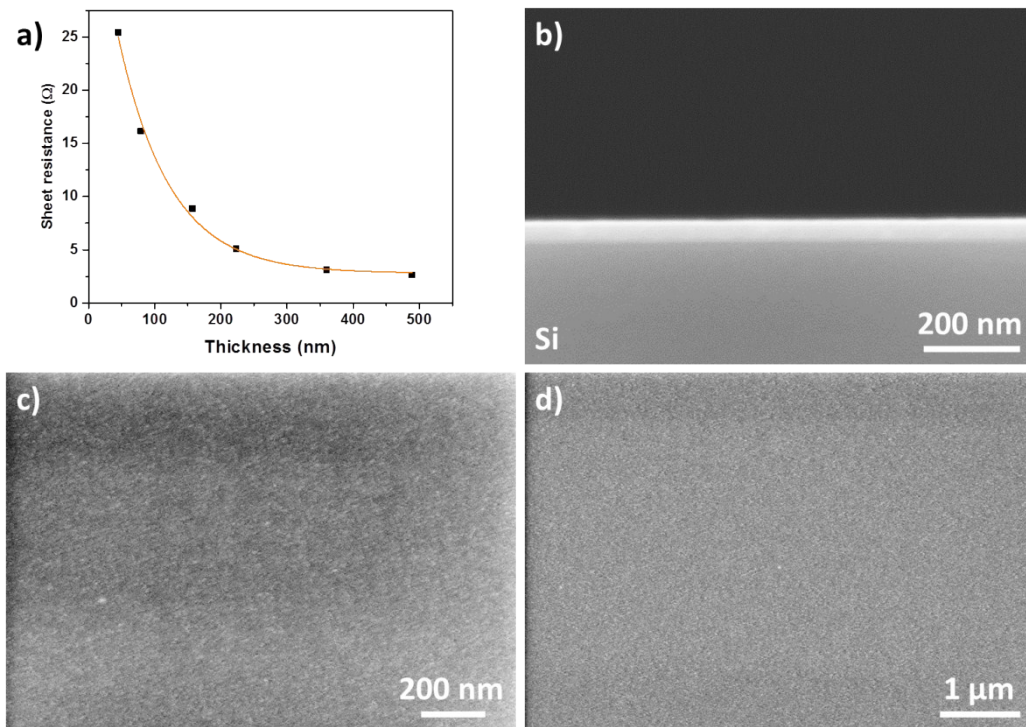


Figure S7. a) Evolution of $\text{Cr}_{2.1}\text{N}$ sheet resistance with thickness. b)-d) SEM micrographs of a 45 nm thick $\text{Cr}_{2.1}\text{N}$ film.

The change in surface microstructure for $\text{Cr}_{2.1}\text{N}$ thin films of 79 nm to 489 nm is presented in Fig. S8.

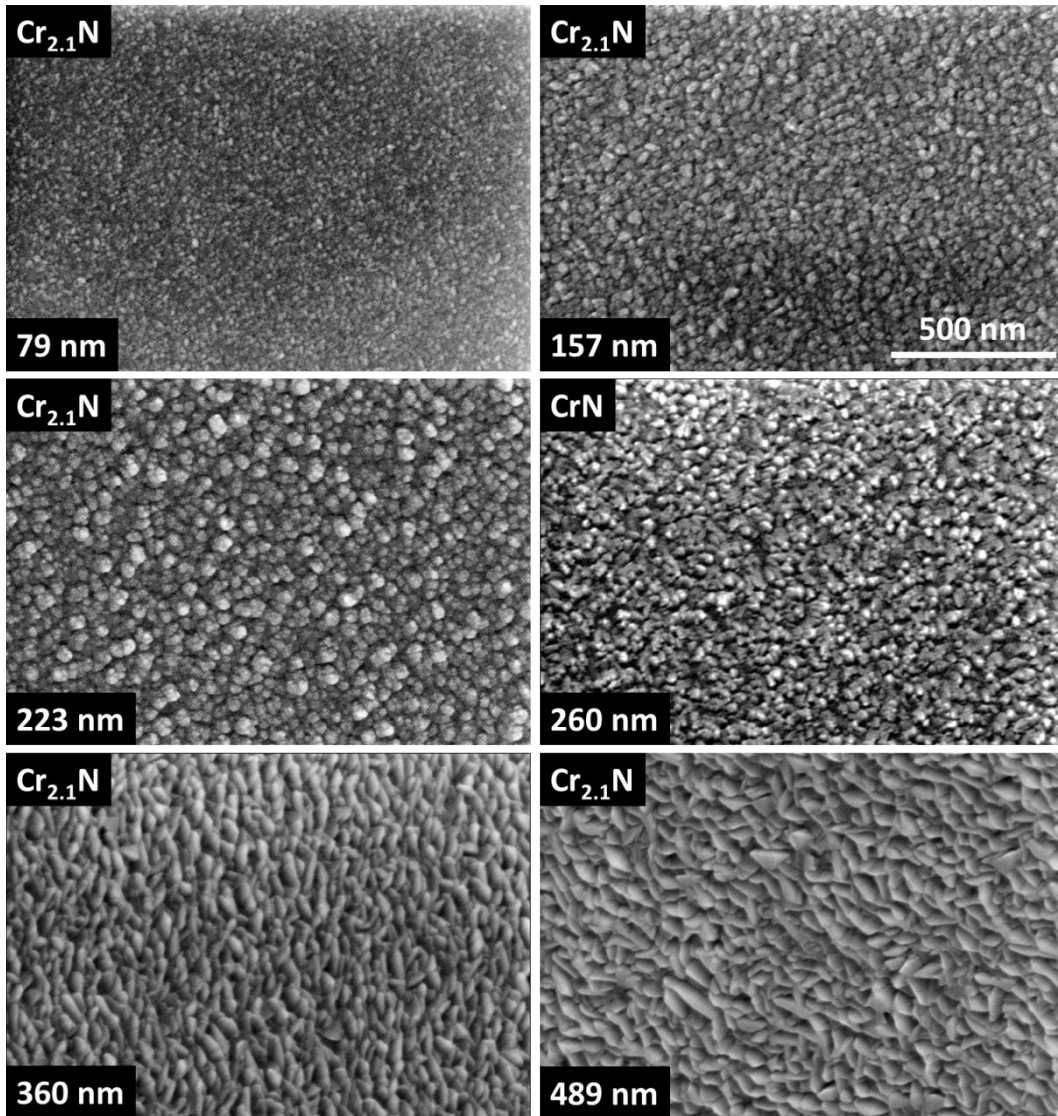


Figure S8. SEM normal views of $\text{Cr}_{2.1}\text{N}$ with different thicknesses. A 260 nm thick CrN film has been included for comparison.

The morphology of as-prepared LMNO/ Cr_2N /Si samples can be seen in Fig. S9.

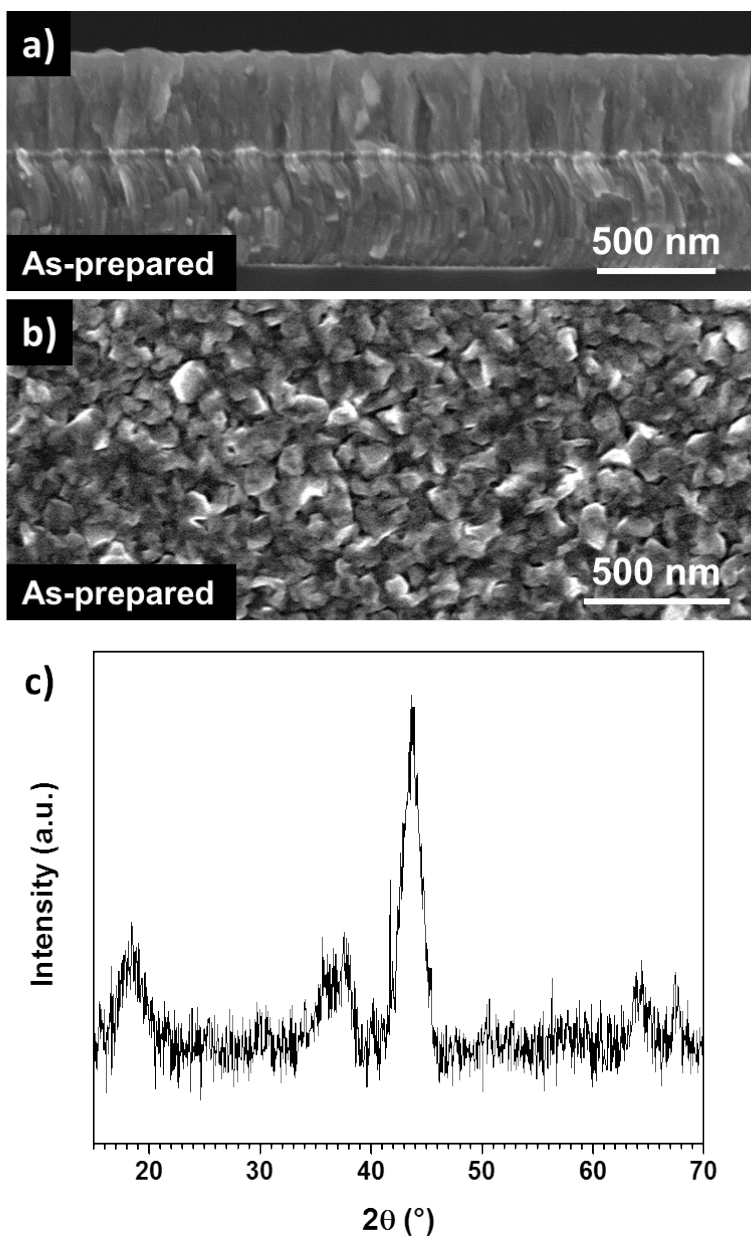


Figure S9. SEM normal view of as-prepared LMNO(500) on Cr₂N(500 nm)/Si (a) and its cross section (b). c) GIXRD of as-prepared LMNO(500 nm)/Cr₂N(500 nm)/SS at $\omega = 1^\circ$.

Upon annealing the surface of the samples develops crystals which size depends on the annealing temperature, observing the largest crystal for the 700 $^\circ$ C 1 hour treatment, which might be attributed to the large surface segregation of chromium (Fig. S10).

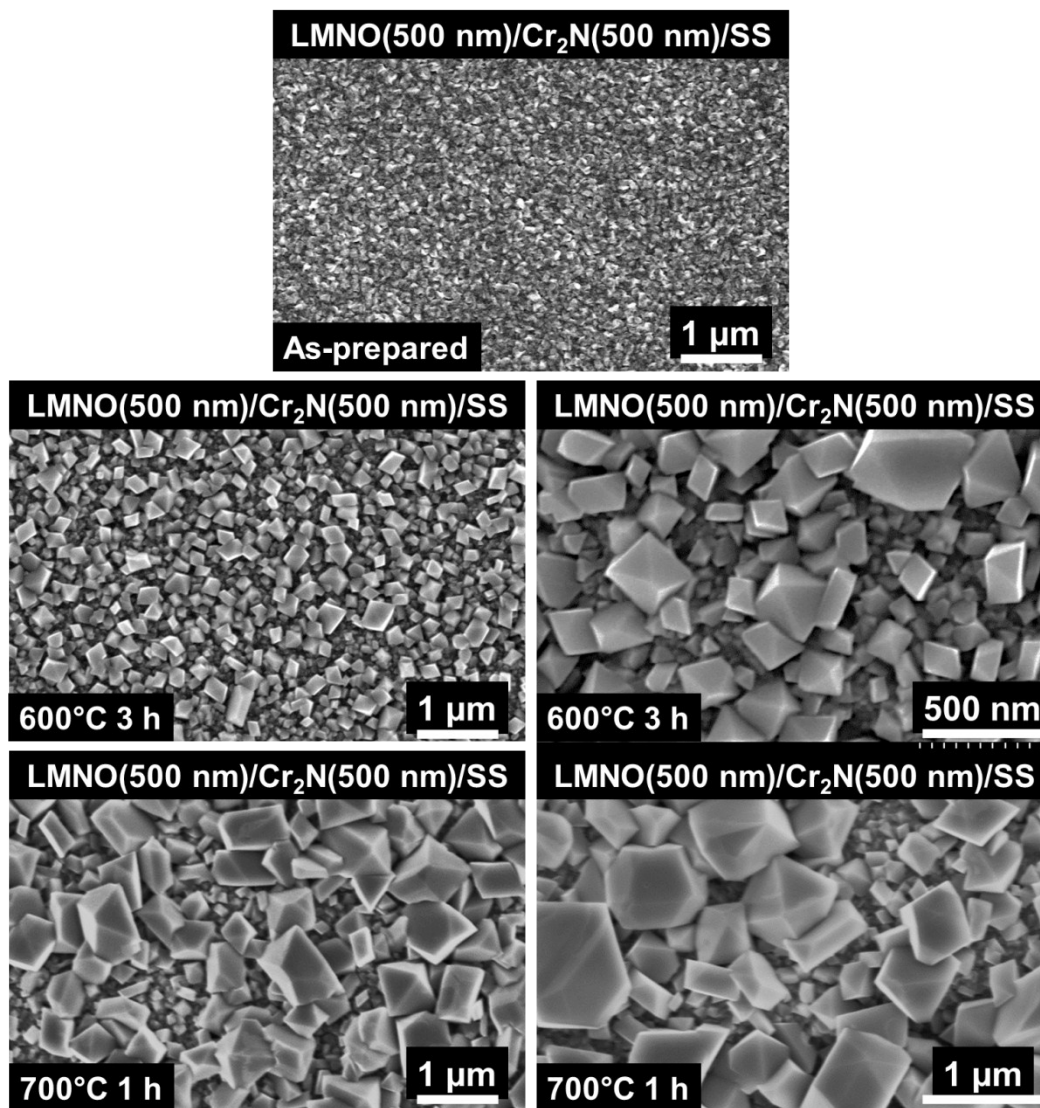


Figure S10. SEM normal views of LMNO(500 nm)/Cr₂N(500 nm)/SS for the as-prepared (top), 600 °C 3 h (middle) and 700 °C 1h (bottom) cases.

The morphology of LMNO/Cr₂N/Si annealed at 700 °C for 1 hour can be seen in Fig. S11.

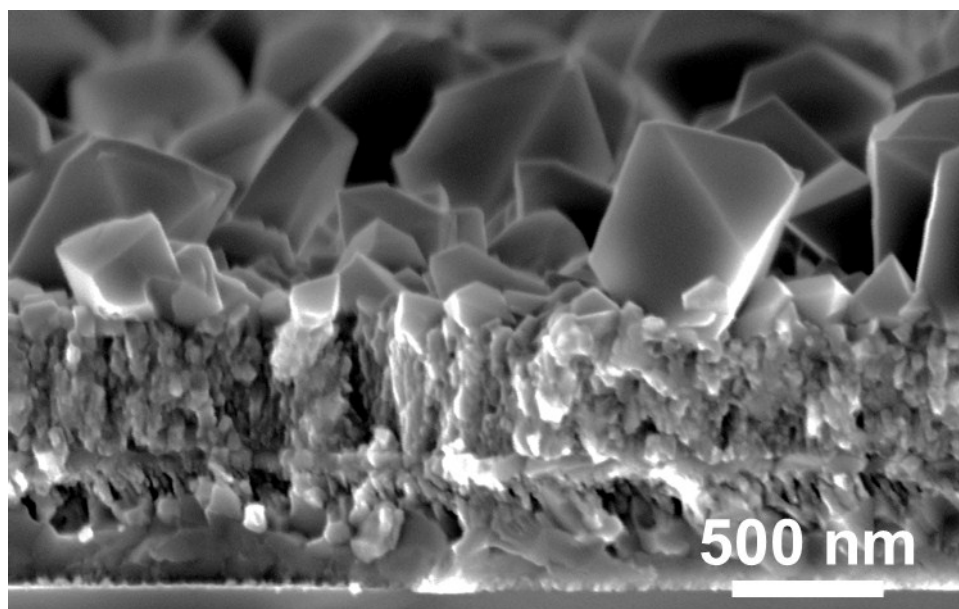


Figure S11. SEM cross section of LMNO(500 nm)/Cr₂N(500 nm)/Si annealed at 700 °C 1 hour.

Figure S12 gathers the XPS surveys for some relevant samples. Please notice that the Na and Ca originally present in the survey of sample LMNO(500 nm)/Cr₂N(500 nm)/Si at 600 °C is due to impurities in the first target that decreased upon target usage.

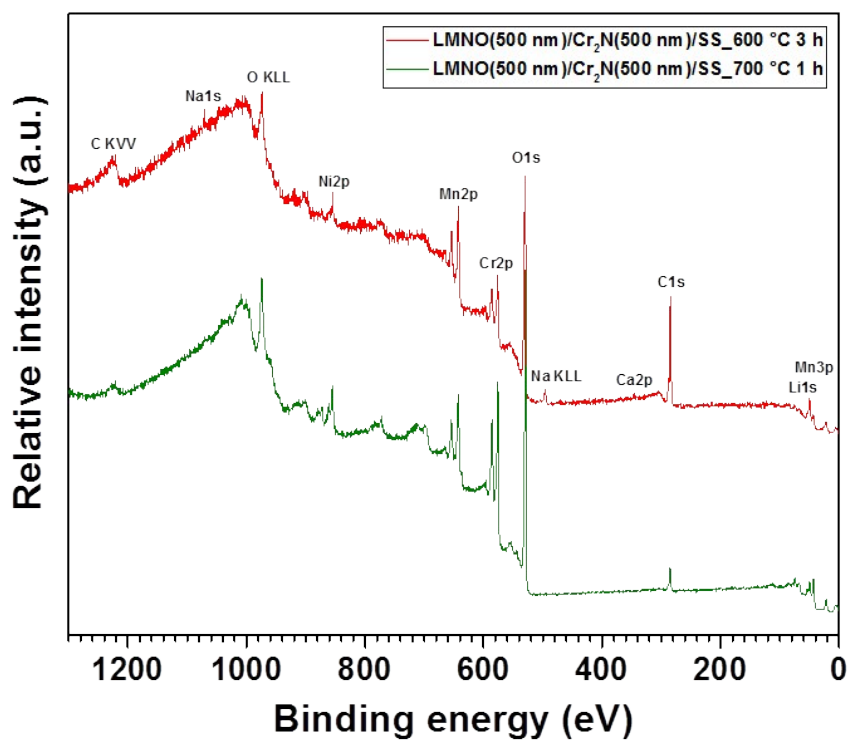


Figure S12. XPS surveys of the samples LMNO(500 nm)/Cr₂N(500 nm)/SS annealed at 600 °C for 3 hours and annealed at 700 °C 1 hour.

LMNO(500 nm)/Cr₂N(500 nm)/SS 600 °C 3 h

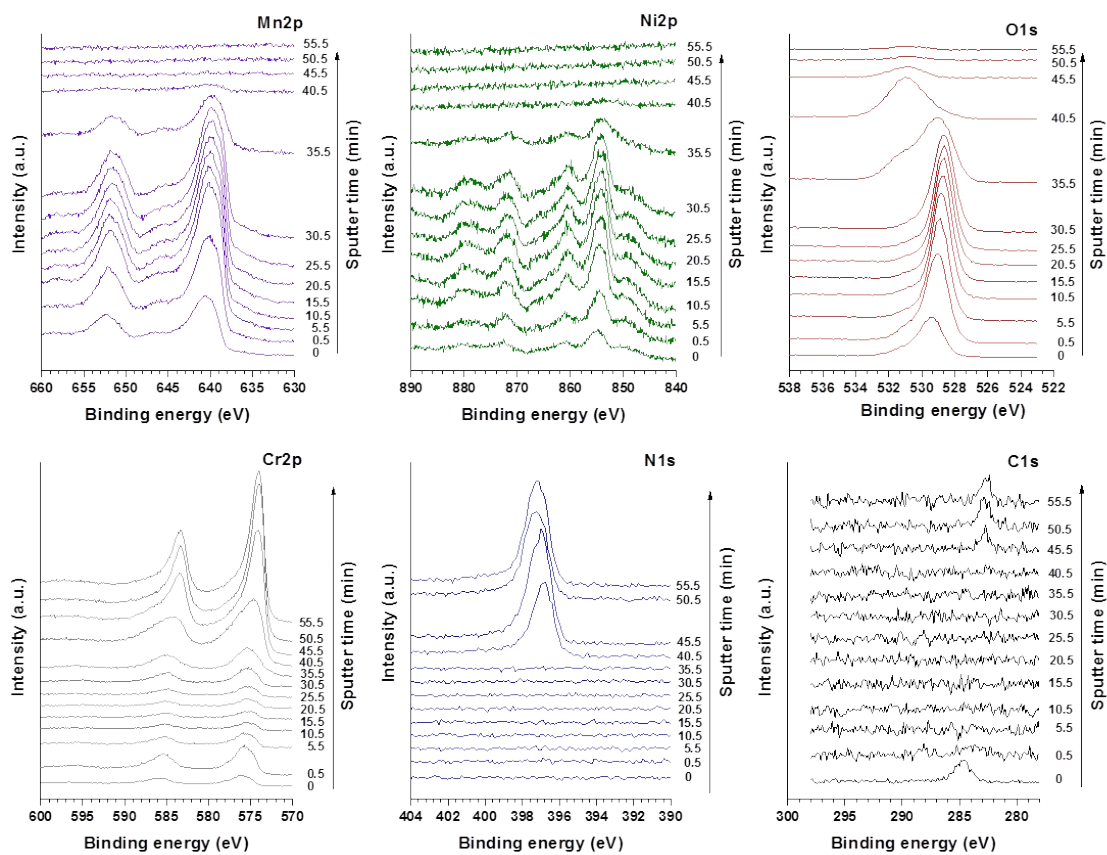


Figure S13. XPS peaks for several elements in the sputter-depth profile of LMNO(500 nm)/Cr₂N(500 nm)/SS, annealed at 600 °C for 3 hours.

LMNO(500 nm)/Cr₂N(500 nm)/SS 700 °C 1 h

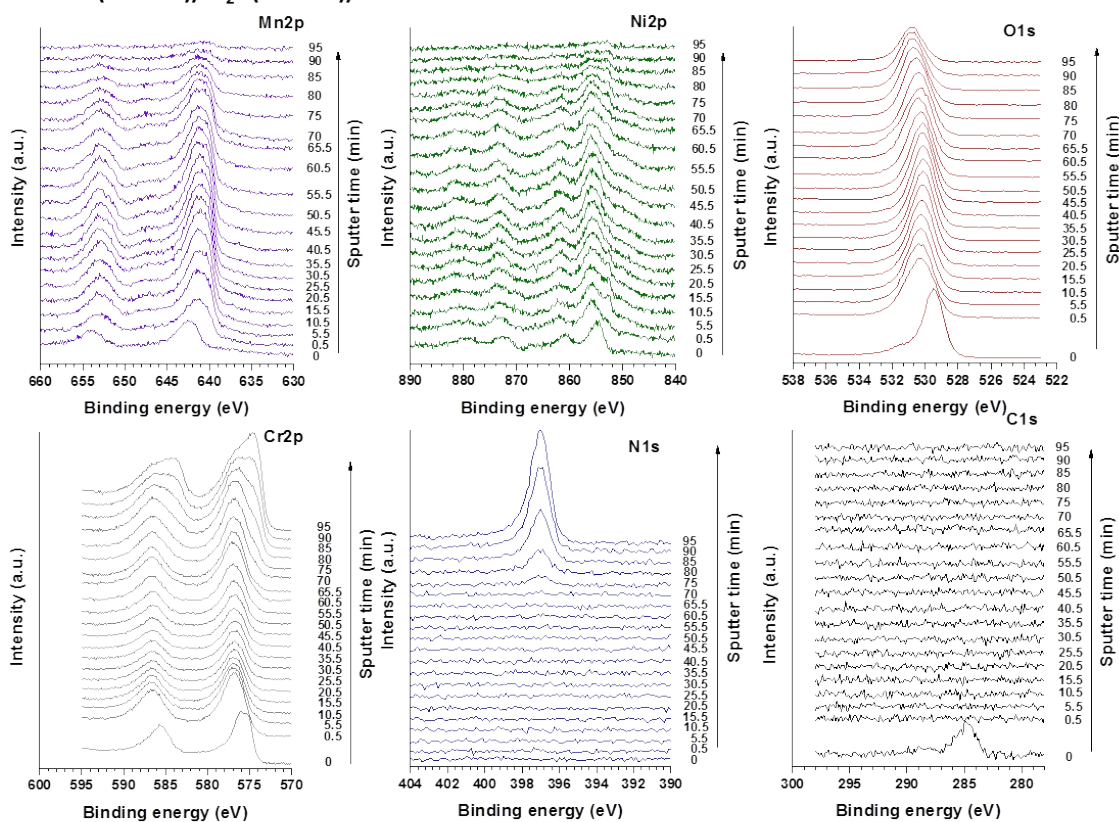


Figure S14. XPS peaks for several elements in the sputter-depth profile of LMNO(500 nm)/Cr₂N(500 nm)/SS, annealed at 700 °C for 1 hour.

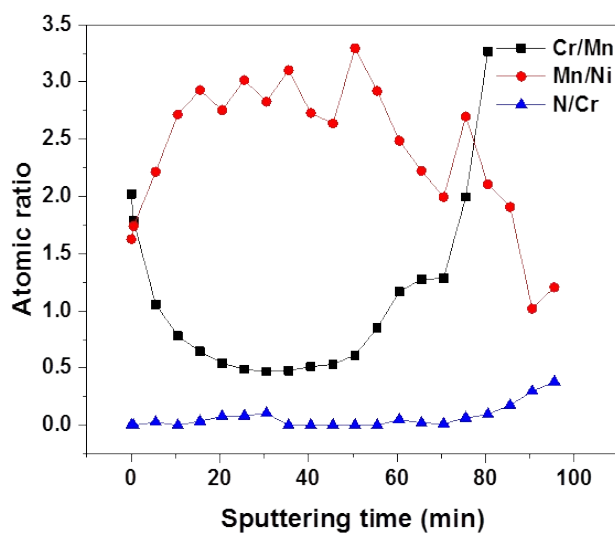


Figure S15. Mn/Cr, Mn/Ni and N/Cr atomic ratios for LMNO(500 nm)/Cr₂N(500 nm)/SS after annealing at 700 °C 1 hour calculated from Fig. S17.

